

Introduction: Calcium–aluminum-rich inclusions (CAIs) are a type of coarse-grained clast composed of Ca-, Al-, Ti- and Mg-rich silicates and oxides found in chondrite meteorites. Type B (CAIs) are exclusively found in the CV chondrite meteorites and are the most well studied type of inclusion found in chondritic meteorites. Type B1 CAIs are distinguished by a nearly monomineralic rim of melilite that surrounds an interior predominantly composed of melilite, fassaite (Ti and Al-rich clinopyroxene), anorthite, and spinel with varying amounts of other minor primary and secondary phases.

The formation of Type B CAIs has received considerable attention in the course of CAI research and quantitative models, experimental results and observations from Type B inclusions remain largely in disagreement. Recent experimental results and quantitative models have shown that the formation of B1 mantles could have occurred by the evaporative loss of Si and Mg during the crystallization of these objects [1,2]. However, comparative studies suggest that the lower bulk SiO₂ compositions in B1s result in more prior melilite crystallization before the onset of fassaite and anorthite crystallization leading to the formation of thick melilite rich rims in B1 inclusions [3]. Detailed petrographic and cosmochemical studies of these inclusions will further our understanding of these complex objects.

Petrology and Mineral Chemistry: EK-459-5-1 is a Type B-1 calcium aluminum-rich inclusion in the Allende CV3 carbonaceous chondrite (Figure 1a). The CAI consists of a coarse grained interior portion of melilite, fassaite, spinel and anorthite surrounded by a nearly monomineralic mantle of melilite. The CAIs interior is segregated into zones of spinel free areas rimmed by aggregates of spinel, analogous to spinel palisades, with clumps of coarse grained spinel regions (spinel frambooids); however, fassaite, melilite and anorthite display a uniform distribution throughout the interior.

The melilite mantle is composed of coarse grained melilite laths (Figure 1b) with long lengths roughly oriented from interior to exterior across the melilite mantle. Major element oxide compositions typically show a pattern of increasing Åkermanite number (Åk#) toward the interior of the CAI. In certain portions of the mantle, for several hundred micrometers from the interior portion toward the exterior of the melilite man-

tle, narrow bands of oscillating Åk# in melilite occurs, where sharp increases followed by decreases in Åk# are observed in a periodic fashion with Åk# peaks occurring approximately every 50-100 μ m. This zone of oscillatory Åk# in the melilite mantle is referred to here as the oscillatory zone (OZ; Figure 1c) and commonly small fassaites occur in bands parallel to the OZ in

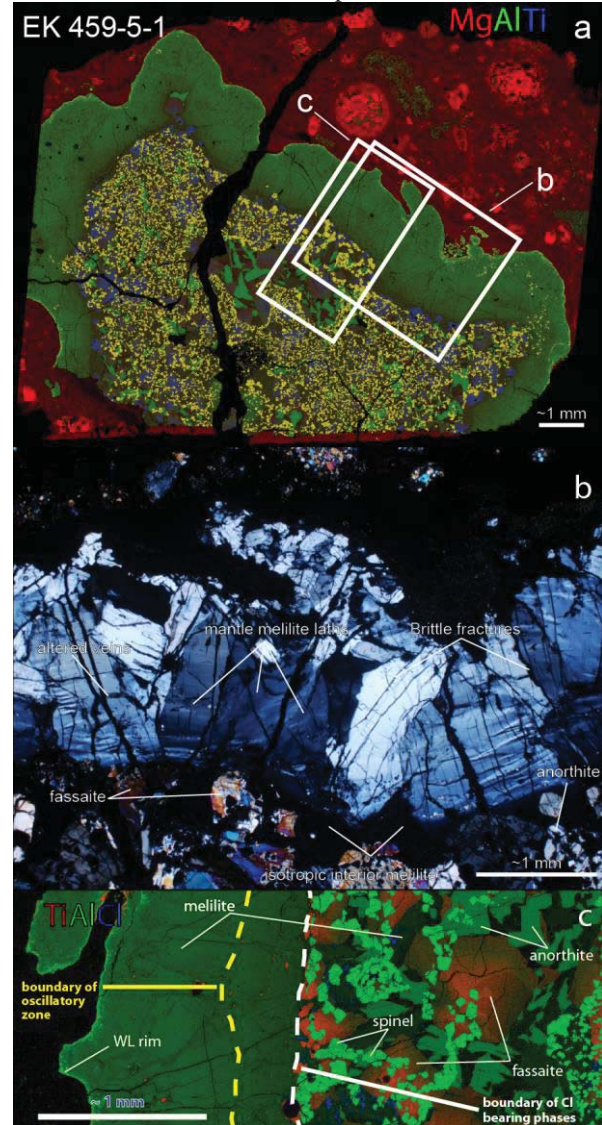


Figure 1: EK-459-5-1 thin-section images: a) X-Ray three element EDS map (Mg-Red, Al-Green, Ti-Blue) of the entire inclusion, b) Optical photomicrograph in XPL of a close up of the mantle rim, c) X-Ray three element EDS map (Ti-Red, Al-Green, Cl-Blue) of a portion of mantle and interior.

localized Åk# low regions. X-ray elemental maps (Figure 1c) show the OZ bands are not uniformly distributed throughout the entire mantle-interior boundary.

Melilite in the interior of the CAI occur as euhedral to subhedral, blocky to equant grains and commonly possess fractures or veins of a fine-grained, Cl-bearing aggregate similar to the mineral filled veins in the melilite mantle portions. A ubiquitous feature of the relationship between melilite in the interior and anorthite is the formation of the fine-grained mesostasis along shared grain boundaries. Major element compositions of melilite display symmetric zoning from core to rim with high Åk# contents ($\sim\text{Åk}_{57-60}$) in the center and slightly decrease toward the rim to minimum values of $\sim\text{Åk}_{50-52}$.

Aluminum and titanium rich augite (fassaite) occurs as euhedral to subhedral, equant grains. Many grains of fassaite are poikilitic with small inclusions of spinel and occasionally melilite guests in the interior most regions of larger crystals. Small fassaite crystals occur in the melilite mantle particularly within OZ near the mantle-interior boundary. Additionally, very small fassaite grains are observed near the rims of some spinel grains. Major element compositions of fassaite display strong compositional zoning with respect to major and trace elements. Fassaite cores possess higher concentrations of Al, Ti, V, and Sc that decrease gradually toward the rim. Si, Mg, Y and the REEs display reverse zoning behavior with lower concentrations in the cores and increasing gradually toward the rim. Sector zoning is present in nearly all fassaite grains. Sector zoning is marked by sharp changes in the concentration of Al_2O_3 , SiO_2 and MgO up to 5 wt.% over $<1\ \mu\text{m}$ distances. $\text{Ti}^{3+}/\text{Ti}^{\text{tot}}$ concentrations for fassaite grains display two patterns: 1) those that are zoned with decreasing concentrations of $\text{Ti}^{3+}/\text{Ti}^{\text{tot}}$ from core to rim, and 2) those that show only slight or no zoning with respect to $\text{Ti}^{3+}/\text{Ti}^{\text{tot}}$ values from core to rim. Those fassaites that are closest to the melilite mantles are the ones that display no zoning in $\text{Ti}^{3+}/\text{Ti}^{\text{tot}}$ values whereas those that are the interior most fassaite grains display the strongest $\text{Ti}^{3+}/\text{Ti}^{\text{tot}}$ zoning profiles.

Discussion: EK-459-5-1 bulk compositions for the whole CAI plotted on the anorthite, gehlenite and forsterite ternary projected from spinel indicate 30% to 40% evaporation of Mg from the precursor condensate compositions calculated by [4]. Asymmetric zoning in the melilite mantle may be explained in two ways: 1) outside-in growth with the most Al-rich component crystallizing first [5] or 2) evaporative loss of SiO_2 and MgO during partially molten stages [2]. Asymmetric zoning in interior melilite crystals may be due to only certain portions of the crystal being in contact with the melt or melt pocket from which the crystal is growing [3]. In this situation the zoning is more likely caused

by fluctuations in the localized melt pocket's Al/Mg ratio as crystallization proceeds. Reverse zoning in interior melilite may be caused by slow cooling rates ($<50^\circ\text{C}/\text{hr}$) where anorthite nucleation is suppressed and the cocrystallization of fassaite and melilite drives the Al/Mg ratio of the melt up increasing the gehlenitic component of melilite [6].

Sector zoning may be preserved in pyroxenes, if crystal growth rates are relatively fast compared to rates of diffusion within the crystal, and sector zoned fassaites (Ti-rich pyroxenes) are common in Type B2 CAIs but rare in Type B1 inclusions [3]. Since crystallization temperatures for both B1 and B2 inclusions are nearly identical, diffusion rates between the two inclusion types would be similar and therefore, it was likely B2 fassaites had faster growth rates than B1. Additionally, higher bulk SiO_2 compositions and greater pyroxene components in B2 inclusions coupled with less prior crystallization of melilite could have facilitated faster growth rates in B2 inclusions than B1 inclusions. Bulk SiO_2 compositions for EK-459-5-1 (~ 28 wt %) fall within the typical range for B1 CAIs and are lower than typical bulk analyses for Type B2 inclusions; therefore, it is unlikely that sector zoning resulted from a compositional difference in this inclusion. It is more reasonable that the sector zoning in the fassaites from EK-459-5-1 was the result of faster crystal growth within this inclusion compared to other Type B1 CAIs. In EK-459-5-1 only fassaites near the melilite mantle, and outermost regions of the interior, are unzoned with respect to $\text{Ti}^{3+}/\text{Ti}^{\text{tot}}$ values. Grains in the interiormost region of the inclusion tend to be strongly zoned with respect to $\text{Ti}^{3+}/\text{Ti}^{\text{tot}}$. It is possible that the grains near the melilite rim could have still been able to be in equilibrium with the surround gas.

Conclusions: EK-459-5-1 is a Type B1 CAI that harbors many common characteristics of other Type B1 CAIs; however, some uncommon features have been observed. Asymmetric melilite zoning features suggest that melilites zoning arose due to the crystal only growing into a melt pocket from one direction. Additionally, cocrystallization of fassaite and melilite followed by late anorthite crystallization may have caused the asymmetric zoning patterns in interior melilite. The sector zoning observed in fassaite is likely caused by increased crystal growth rates as opposed to differences in the bulk SiO_2 compositions.

References: [1] Richter, F.M. et al. (2002), *GCA*, 66, 521–540 [2] Mendybaev, R. et al. (2006) *GCA*, 70, 2622–2642, [3] Simon, S.B. and Grossman, L. (2006) *GCA*, 70, 780–798, [4] Grossman, L. et al. (2000) *GCA*, 64, 2879–2894, [5] Wark, D.A. and Lovering, J. F. (1982) *GCA*, 46, 2581–2594, [6] Macpherson, G.J. et al. (1984) *J. Geol.*, 92, 289–305.